Active Cancellation of the Occlusion Effect in Hearing Aids by Time Invariant Robust Feedback

Stefan Liebich, Peter Jax, Peter Vary

Institute for Communication Systems
RWTH Aachen University
52074, Aachen
Email: {liebich,vary,jax}@iks.rwth-aachen.de
Web: www.iks.rwth-aachen.de

Abstract

The hollow perception of the own voice is still one of the major problems of hearing aids. This "occlusion effect" (OE) occurs when the ear canal is completely covered and manifests as an amplification of low frequency components. We are investigating the compensation of this effect by active noise cancellation (ANC). A time-invariant feedback controller, corresponding to a digital filter, is designed by the mixed-sensitivity $\mathscr{H}_\infty$ controller synthesis. The secondary path, describing the transmission between internal loudspeaker and internal microphone, is of great importance. The synthesis requires models of this secondary path, its uncertainty and an objective function for the desired overall system transfer function. The objective function is fitted to the individual OE. The design and the evaluation within simulations include acoustical measurements of the real paths.

The novelty is the specific consideration of the OE and the uncertainty of the secondary path within the optimization process.

1 Introduction

The acceptance of hearing aids by their users is degraded by various influences, very prominently by the occlusion effect (OE) [15]. It occurs in the case of a covered ear canal, as present in closed-fitted hearing aid applications. The sensation of this effect is mostly described as hollow [6]. Objectively, it can be measured as an amplification of low frequency components of the own voice within the ear canal.

This problem has been addressed by hearing aid manufacturers since decades. Two mechanical approaches, namely venting and deep fitting, have shown their effectiveness, but carry other disadvantages. For venting, a ventilation hole is integrated into the earmold [15], which unfortunately increases the feedback between the inner loudspeaker and the outer microphone. For deep fitting, the earmold is inserted very deeply into the canal itself, which negatively affects the wearing comfort [15].

A new approach has recently revealed promising results in research. Active noise cancellation (ANC) can be used to create an "electronic vent" without increasing the feedback problem. In the last decade, a few attempts have been made using fixed, i.e. time-invariant, feedback controllers [15], [7], [8], [13] or adaptive approaches [2], [14]. Though, the fixed feedback controller was tuned manually in all publications addressing it. A specific optimization of the ANC attenuation for the OE, was not addressed so far. Furthermore, the influence of the acoustic front-end and thereby the secondary path was largely disregarded. More focus on the acoustic front-end has recently been put by [13], investigating a stacked receiver-microphone combination. However, the influence of uncertainty within the secondary path, was not explicitly considered so far. In this publication we are designing a feedback controller with a sensitivity, i.e. the overall transfer function of the system, inverse compared to the OE and explicitly consider the path uncertainties.

2 Occlusion Effect

The hollow sensation of one's own voice results from two major influences. First, the perception of the own voice is always a combination of mainly two signals (regarding the outer ear influence). These are the well-known outer, air-conducted (AC) component, $x'_{\text{AC}}(t)$[1], and the inner, bone-conducted (BC) component, $x'_{\text{BC}}(t)$, as illustrated in Fig. 1. This combination is also the reason why the perceived own voice differs from recordings. Second, the earmold occludes the ear canal and therefore changes the acoustic terminating impedance of it [15]. From the outside, especially the high frequencies of $x'_{\text{AC}}(t)$ are attenuated by the earmold. From the inside, the low frequency components induced by the bone conduction signal $x'_{\text{BC}}(t)$ cannot escape the ear canal. This leads to amplified low frequency components, in extreme cases by up to 30 dB [12].

The frequency-dependent OE can be quantified by the ratio of the signal $d'(t)$ at the eardrum with and without the occlusion.

$$OE(f) = \frac{|D'_{\text{occl}}(f)|}{|D'_{\text{open}}(f)|}. \tag{1}$$

However, this ratio cannot be measured due to a non-reproducible excitation signal with the own voice. Therefore, we consider the occlusion function

$$\widetilde{OE}(f) = \frac{|D'_{\text{occl}}(f)|}{|X'_{\text{AC}}(f)|}, \tag{2}$$

which disregards the influence of the ear canal on the open ear signal [15]. One approach to measure this latter ratio is described in Sec. 4.3.

3 Robust Active Noise Control

The structure of the ANC system for the OE compensation is illustrated in Fig. 1. The acoustic disturbance signal[2] $d'(t)$ is a combination of an AC and a BC part of the own voice excitation with the influence of the earmold as described in Sec. 2. Furthermore, $x'_{\text{AC}}(t)$ contains ambient sounds, which are of minor interest in this application and neglected here.

[1] For simplicity we use the same names for discrete time k and continuous time t variables e.g. $e(t)$ and $e(k) = e(kT)$ or $G(s) = \mathscr{L}\{g(t)\}$ and $G(z) = \mathscr{Z}\{g(k)\}$, whereas $z = e^{sT}$.

[2] Acoustic signals are marked by $'$.

ISBN: 978-3-8007-4275-2

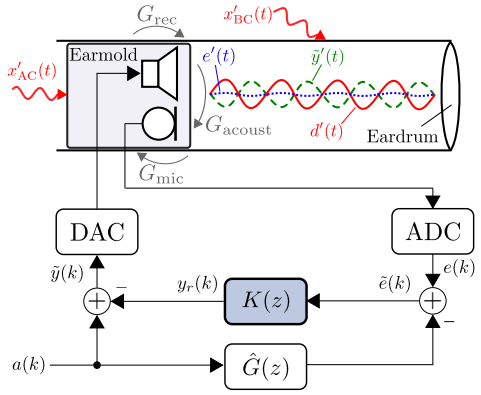

Figure 1: Digital implementation of an ANC system connected to a hearing aid with an additional internal microphone.

This inner disturbance signal $d'(t)$ is measured via a microphone and a controller $K(z)$ creates a cancellation signal $y_r(k)$, which is played back via the loudspeaker, often addressed as *receiver* in the area of hearing aids. The receiver-to-microphone transfer function is concentrated within the secondary path $G(s)$, also known as the *control plant* in control theory. It includes their characteristics $G_{\text{rec}}(s)$ and $G_{\text{mic}}(s)$, the analog-digital-conversion (ADC), the digital-analog-conversion (DAC) and the acoustic transmission $G_{\text{acoust}}(s)$. Usually, we desire to play back an additional audio signal $a(k)$, e.g. a processed version of the outer sound signal $x'_{\text{AC}}(t)$ for hearing aids, which is neglected here and only mentioned for completeness.

The goal is to design a controller $K(z)$ to compensate the OE. To construct this controller, we use the so-called mixed-sensitivity $\mathscr{H}_\infty$ controller synthesis, as introduced e.g. in [11]. For describing the overall system and its performance, we consider the sensitivity function $S(s)$ as well as the complementary sensitivity function $T(s)$. The sensitivity function

$$S(s) = \frac{1}{1+G(s)K(s)} \tag{3}$$

reflects the influence of the disturbance $d(t)$ on the residual signal $e(t)$. It therefore represents the overall system attenuation. The complementary sensitivity function

$$T(s) = \frac{G(s)K(s)}{1+G(s)K(s)} \tag{4}$$

on the other hand describes the influence of the disturbance $d(t)$ on the secondary path output $y(t)$. $T(s)$ gives an indication on the robustness of the system. These two sensitivity functions are connected by the so called dilemma of feedback control [11]

$$S(s)+T(s) = 1. \tag{5}$$

Therefore, we always need to make a trade-off between performance and robustness.

Within the controller synthesis, we want to shape these two transfer functions $S(s)$ and $T(s)$ by designing an appropriate $K(s)$. For this we are using the mixed-sensitivity $\mathscr{H}_\infty$ synthesis, which requires an augmented plant as shown in Fig. 2. The plant is extended by three frequency-dependent

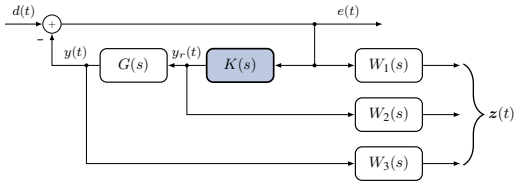

Figure 2: Feedback Control System with mixed-sensitivity weighting functions W_1 to W_3 without additional audio signal (taken from [10]).

weighting functions $W_i(s)$ with $i = 1..3$. The transfer function between the disturbance $d(t)$ and the combined output $\boldsymbol{z}(t)$ yields

$$\boldsymbol{T}_{zd}(s) = \begin{bmatrix} W_1(s)S(s) \\ W_2(s)K(s)S(s) \\ W_3(s)T(s) \end{bmatrix}. \tag{6}$$

We look for the controller $K(s)$ to minimize the $\mathscr{H}_\infty$-norm [11] of this transfer function, which takes the value γ precisely

$$\min_K \|\boldsymbol{T}_{zd}(s)\|_\infty = \min_K \gamma. \tag{7}$$

Within the design process, the weighting functions W_i may be chosen to affect the outcome of the optimization. They must be proper and stable. $W_1(s)$ is the sensitivity objective function that represents the desired overall system attenuation and is chosen according to $1/\widetilde{OE}(f)$. We are designing a fixed controller and therefore need to consider uncertainties in $G(s)$ resulting from individual variations in the ear canal and the occlusion. These uncertainties in $G(s)$ are described within $W_3(s)$. $W_1(s)$ is usually chosen in relation to $W_3(s)$, as the possible performance is strongly influenced by the uncertainty. As we only want to shape $S(s)$ and $T(s)$, we set $W_2(s) = 0$ and neglect the second output of is this more general mixed-sensitivity approach.

4 Controller Design

The general design of an ANC controller was already described in [10] and is only shortly repeated in this paper. Due to the analog nature of the real system, it is reasonable to also design the controller in a continuous form. We therefore use the $\mathscr{H}_\infty$ optimization procedure in the Laplace domain. For this we need continuous models of $G(s)$, $W_1(s)$ and $W_3(s)$. The estimation and design of these models is described in the following.

For all following illustrations we are regarding the dependency on the frequency $\omega = 2\pi f$. We therefore evaluate $s = j\omega = j2\pi f$ and $z = e^{j2\pi f/f_s}$.

All measurements for the design were done with one male proband A. We used a *Bose QC 20* in-ear headphone hardware as the acoustic front-end [1], connected to a dSPACE real-time system (DS1005, dSPACE GmbH, Paderborn, Germany) with the DS2004 AD-extension and the DS2102 DA-extension board. The acoustic front-end did not include any explicit venting. The round trip delay of this system, including the DAC and the ADC, but excluding the acoustics, is 1 sample at a sampling rate of $f_s = 48\,\text{kHz}$.

4.1 Secondary Path Modelling

For a suitable controller design, we need knowledge about the acoustic secondary path $G(s)$. We measured it with digital logarithmic sweep signals [9] to create a time-discrete

ISBN: 978-3-8007-4275-2

version $G_{\text{meas}}(z)$. Proband A was wearing the in-ear headphone during these measurements in his right ear. The model order of this discrete model is decreased by the prediction error minimization method to get an ARMA model $G(z)$ and it is transformed into the Laplace domain to acquire $G(s)$ of model order 15 (linear interpolation / first-order hold method) [11]. The magnitude and phase response are shown in Fig. 3.

4.2 Modelling the Uncertainty

The acoustical secondary path is naturally afflicted by an uncertainty. In order to guarantee stability of the feedback system, this uncertainty needs to be taken into account within the controller design. We include the uncertainty in the perturbed path $G_{\text{p}}(s)$ in a multiplicative form [11]:

$$G_{\text{p}}(s) = G(s) \cdot (1 + W_{\text{M}}(s)\, \triangle_{\text{I}}(s)) \text{ with } |\triangle_{\text{I}}(j\omega)| \leq 1 \forall \omega, \tag{8}$$

and $|W_{\text{M}}(j\omega)|$ being the measured uncertainty bound. Resulting from the stability conditions within the Nyquist diagram, the absolute inverse of $|W_{\text{M}}(j\omega)|$ needs to be always greater than the absolute values of the complementary sensitivity for all frequencies to guarantee robust stability [11]. Precisely

$$|T(j\omega)| < 1/|W_{\text{M}}(j\omega)|, \forall \omega. \tag{9}$$

To determine this uncertainty bound $|W_{\text{M}}(j\omega)|$, we conducted measurements of typical use cases with proband A (tight/loose fit), as well as everyday situations (lying on a table, covered housing canal). The relative deviation of these measured paths $\tilde{G}(j\omega)$ from the desired secondary path $G(j\omega)$ is given as

$$E_G(j\omega) = \frac{\tilde{G}(j\omega) - G(j\omega)}{G(j\omega)}. \tag{10}$$

Thereafter, we calculated $|W_{\text{M}}(j\omega)|$ by

$$|W_{\text{M}}(j\omega)| = \max_{\tilde{G}} |E_G(j\omega)|. \tag{11}$$

Furthermore, we modified the uncertainty to manipulate the optimization in a positive way. For low and high frequencies, the uncertainty is increased, as the microphones give less accurate results in these regions. The reciprocal magnitude of the uncertainty $W_{\text{M}}(s)$ and the modified uncertainty $W_3(s)$ are shown in the lower plot of Fig. 5 as dashed lines. The final model $W_3(s)$ has an order of 13 in state-space form.

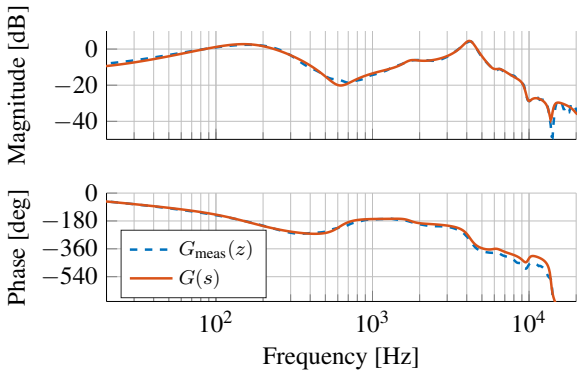

Figure 3: The magnitude and phase responses of the secondary path with both the discrete measurement $G_{\text{meas}}(z)$ and the model $G(s)$ of order 15.

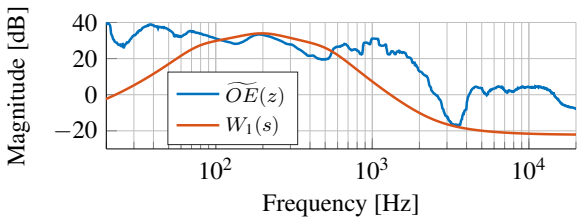

Figure 4: Measured OE represented by $\widetilde{OE}(z)$ and the simplified weighting function $W_1(s)$.

4.3 OE Depending Sensitivity Bound

Our goal is to construct a controller that compensates the OE and therefore has a sensitivity function $S(s)$ inverse compared to $\widetilde{OE}$. This may be achieved by defining the sensitivity objective $W_1(s)$ according to $1/\widetilde{OE}$. For the measurement we are using the *Oldenburg* setup with two miniature microphones from Knowles (FG-23329-P07) [15]. Both microphones have been calibrated relative to each other. Then the proband is asked to pronounce an [*i* :], which results in a very strong OE. The OE is calculated by spectral division following Eq. 2 and smoothed by an 1/3-octave band average filter. To contain the complexity of the final controller $K(s)$, we created a simplified model $W_1(s)$ of order 6. Both are shown in Fig. 4. The weighting functions $W_1(s)$ and $W_3(s)$ are typically mutually chosen.

4.4 Optimization, Model Reduction and Discretization

Like in [10], we use a state space approach based on the solution of two Riccati equations (ARE) proposed in [3] for solving the optimization problem of Eq. 7. For the implementation in real-time systems, complexity is an issue. Therefore, we reduce the model order by the use of Hankel singular values, which represent the energy of each state of a system in state space form. In our case, we reduced the order of $K(s)$ from 34 to 20 to acquire a lower order model $K_{\text{red}}(s)$. This was realized by truncating the last 14 states with lowest energy, maintaining 99.62% energy in the hankel singular values.

The controller is applied in a digital system and therefore the reduced model is digitalized to create $K(z)$ (linear-interpolation / first-order hold method) [4].

5 Evaluation

In the evaluation we first consider the controller $K(z)$ and the expected performance. Thereafter, we are conducting simulations with real measurements to evaluate the practical performance.

We are using three different secondary path measurements $G_{\text{meas}}(z)$ from two human subjects (male proband A and female proband B) and one dummyhead D (HMS II.3 with 6460 MFE VI amplifier, HEAD acoustics GmbH, Herzogenrath, Germany). The controller was optimized for proband A.

5.1 Controller Evaluation

For evaluating the controller itself, we are considering the measurements from proband A. We are regarding the performance represented by the sensitivity function $S(s)$ and the robustness contained in the complementary sensitivity

ISBN: 978-3-8007-4275-2

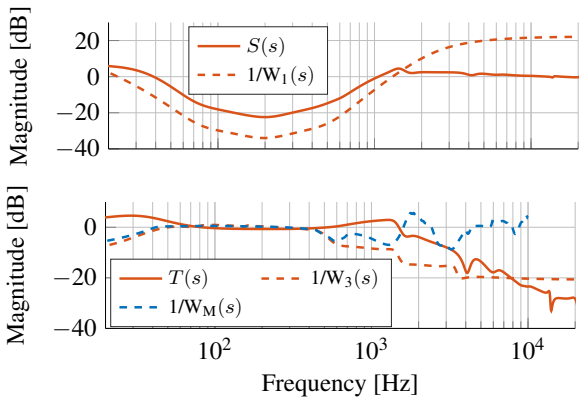

Figure 5: Sensitivity $S(s)$ and the design target, the inverse weighting function $W_1(s)$ (upper); Complementary sensitivity $T(s)$, the design target given by the inverse weighting function $W_3(s)$ and the measured uncertainty $W_M(s)$ (lower).

function $T(s)$. Fig. 5 shows these functions $S(s)$ and $T(s)$ with solid lines, compared to their design constraints in dashed lines. The optimization accomplished all demands, when

$$|S(j\omega)| < 1/|W_1(j\omega)|, \tag{12}$$

$$|T(j\omega)| < 1/|W_3(j\omega)| \tag{13}$$

are fulfilled. Considering the upper plot for the performance analysis, we may observe that we achieve at least 10 dB attenuation in the range from 60 to 700 Hz. However, the ambitious design constraints defined by $1/W_1(s)$ could not be met within the optimization, as Eq. 12 is not fulfilled for all frequencies.

In the lower plot, additional to the design constraints $1/W_3(s)$, we illustrated the measured uncertainty $1/W_M(s)$, which represent the real uncertainty of $G(s)$. We may observe that the design constraints were not completely met, as Eq. 13 is not achieved. Furthermore, we sacrificed stability to suit the need of attenuation up to 1 kHz, visible especially in the range from 500 to 1500 Hz, where $T(z)$ exceeds the uncertainty $1/W_M(s)$. However, in all simulations conducted (multiple users, dummyhead, scenarios outline Sec. 4.2), the controller remained stable.

One very common technique to determine the stability of the controller is the gain margin GM and the phase margin PM [11]. When considering the discrete open loop transfer function $G(z) \cdot K(z)$ in the Nyquist diagram, we achieve $GM = 5.35$ dB and $PM = 41.9°$.

5.2 Simulations

For the evaluation of the controller and the reduction of the OE, we conducted offline simulations with in-ear speech recordings at a sampling frequency of $f_s = 48$ kHz. The signals were recorded with the earlier mentioned Knowles miniature microphones (FG-23329-P07) inside and outside the occluded ear canal. Fig. 6 shows the OE, following Eq. 2 with and without the ANC system working for the vowel [i :]. The goal would be to create a flat curve by processing, which would yield an acoustically transparent earmold. We mainly want to reduce the effect in typical frequency range affected by the OE, namely between 80 to 1000 Hz. We may observe that the OE is reduced considerably in the range between 60 to 700 Hz, especially for proband A.

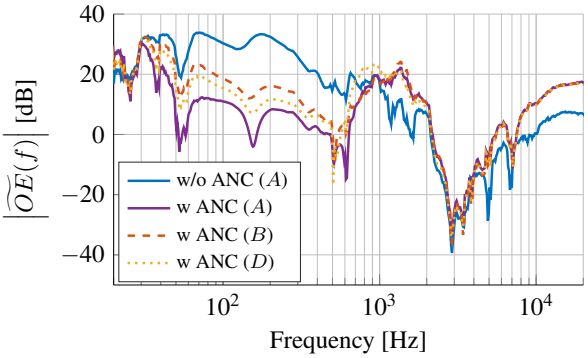

Figure 6: OE for the vowel [i :] without and with ANC for three different secondary paths G - two from human probands (A and B) and one from a dummyhead (D).

The range from 700 to 1000 Hz incorporates still an OE amplification even with ANC. Furthermore, we observe that a variation of the secondary path $G(s)$ leads to a degradation of the controller performance. This degradation may be quantified by the relative error given in Eq. 10, which alters the sensitivity function by [11]

$$\tilde{S}(s) = S(s)\,\frac{1}{1 + E_G(s)T(s)}. \tag{14}$$

In the second simulation a recording of one sentence from the TIMIT database was used (si483) [5]. Fig. 7 shows a short sequence of this sentence to illustrate the ANC performance. We see that the speech signal amplitude is greatly decreased.

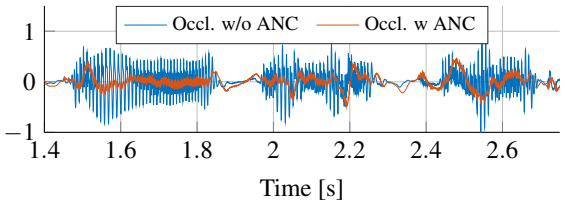

Figure 7: Occluded in-ear signal with and without ANC.

6 Conclusions

The goal was to decrease the OE by an ANC system with a fixed digital controller. This controller is designed by the mixed-sensitivity $\mathscr{H}_\infty$ synthesis, considering actual measurements of the secondary path $G(s)$, its uncertainty represented in $W_3(s)$ and the sensitivity objective $W_1(s)$. This objective function $W_1(s)$ is designed by approximating the actual OE and everyday use cases are taken into account in $W_3(s)$. We designed a controller, for which simulations have revealed a considerable reduction of the OE in the range of 60 to 700 Hz. In the case of mismatches in the secondary path $G(s)$, the occlusion reduction is decreased, however, the controller remains stable. Therefore, the designed system does not require perfect fitting and remains robust in various everyday use cases. However, to achieve optimal performance, the controller needs to be adjusted individually.

ISBN: 978-3-8007-4275-2

References

[1] K. P. Annunziato, J. Harlow, M. Monahan, A. Parthasarathi, R. C. Silvestri, and E. M. Wallace, "In-ear active noise reduction earphone," Patent US8 682 001 B2, 2014. [Online]. Available: https://www.google.com/patents/US8682001

[2] R. Borges, M. Costa, J. Cordioli, and L. Assuiti, "An Adaptive Occlusion Canceller for Hearing Aids," in *IEEE Workshop on Applications of Signal Processing to Audio and Acoustics*, 2013.

[3] J. C. Doyle, K. Glover, P. P. Khargonekar, and B. A. Francis, "State-space solutions to standard H2 and H∞ control problems," *IEEE Transactions on Automatic Control*, vol. 34, no. 8, pp. 831–847, 1989.

[4] G. F. Franklin, J. D. Powell, and M. L. Workman, *Digital control of dynamic systems*. Addison-wesley Menlo Park, 1998, vol. 3.

[5] J. S. Garofolo, *TIMIT: Acoustic-phonetic continuous speech corpus*. [Philadelphia, Pa.]: Linguistic Data Consortium, 1993.

[6] M. C. Killion, "The Hollow Voice Occlusion Effect," in *13th Danavox Symposium*, 1988, pp. 231–241.

[7] J. Mejia, H. Dillon, and M. Fisher, "Acoustically transparent occlusion reduction system and method," Patent WO2 006 037 156 A1, 2006. [Online]. Available: https://www.google.com/patents/WO2006037156A1?cl=en

[8] ——, "Active cancellation of occlusion: An electronic vent for hearing aids and hearing protectors," *Journal of the Acoustical Society of America*, vol. 124, no. 1, pp. 235–240, 2008.

[9] S. Müller and P. Massarani, "Transfer-Function Measurement with Sweeps," *J. Audio Eng. Soc*, vol. 49, no. 6, pp. 443–471, 2001.

[10] S. Liebich, C. Anemüller, D. Rüschen, S. Leonhardt, P. Jax, P. Vary, "Active Noise Cancellation in Headphones by Digital Robust Feedback Control," in *Accepted for publication at EUSIPCO 2016*, 2016.

[11] S. Skogestad and I. Postlethwaite, *Multivariable feedback control: analysis and design*. John Wiley & Sons, 2005.

[12] S. Stenfelt and S. Reinfeldt, "A model of the occlusion effect with bone-conducted stimulation," *Int J Audiol*, vol. 46, no. 10, pp. 595–608, 2007.

[13] M. Sunohara, M. Osawa, T. Hashiura, and M. Tateno, "Occlusion reduction system for hearing aids with an improved transducer and an associated algorithm," in *2015 23rd European Signal Processing Conference (EUSIPCO)*, 2015, pp. 285–289.

[14] M. Sunohara, K. Watanuki, and M. Tateno, "Occlusion reduction system for hearing aids using active noise control technique," *Acoustical Science and Technology*, vol. 35, no. 6, pp. 318–320, 2014.

[15] Thomas Zurbrügg, "Active Control mitigating the Ear Canal Occlusion Effect caused by Hearing Aids," Ph.D. dissertation, EPFL Lausanne, Lausanne, 2014.

ISBN: 978-3-8007-4275-2